Influence of Lipid Saturation Grade and Headgroup Charge: A Refined Lung Surfactant Adsorption Model

U. Klenz, M. Saleem, M. C. Meyer, and H.-J. Galla
Institute of Biochemistry, University of Münster, 48149 Münster, Germany

ABSTRACT Rapid adsorption of surfactant material to the air/liquid interface of the lung is essential for maintaining normal lung function. The detailed mechanism of this process, however, remains unclear. In this study, we elucidate the influence of lipid saturation grade and headgroup charge of surface layer lipids on surfactant protein (SP)-induced vesicle insertion into monolayers spread at the air/water interface of a film balance. We used dipalmitoylphosphatidlycholine (DPPC),1,2-dipalmitoyl-*sn*-glycero-3-phosphoglycerol (DPPG), 1-palmitoyl-2-oleoyl-*sn*-glycero-3-phosphocholine (POPC), and 1-palmitoyl-2-oleoyl-*sn*-glycero-3-phosphoglycerol (POPG) as monolayer lipids doped with either hydrophobic surfactant-specific protein SP-B or SP-C (0.2 and 0.4 mol %, respectively). Vesicles consisting of DPPC/DPPG (4:1, mol ratio) were injected into a stirred subphase to quantify adsorption kinetics. Based on kinetic film balance and fluorescence measurements, a refined model describing distinct steps of vesicle adsorption to surfactant monolayers is presented. First, in a protein-independent step, lipids from vesicles bridged to the interfacial film by Ca^{2+} ions are inserted into defects of a disordered monolayer at low surface pressures. Second, in a SP-facilitated step, active material insertion involving an SP-B- or SP-C-induced flip-flop of lipids occurs at higher surface pressures. Negatively charged lipids obviously influence the threshold pressures at which this second protein-mediated adsorption mechanism takes place.

INTRODUCTION

The pulmonary lung surfactant is a complex lipid-protein monolayer that lines the alveolar air/liquid interface. This surfactant is essential for normal breathing because it lowers the surface tension to about a value of zero and so prevents the collapse of the alveoli (1). During exhalation, it forms tightly packed, meandric multilayer protrusions that can reversibly respread during inhalation (2–5). Furthermore, the surfactant constituents are exchanged continuously. The half-life of different surfactant components is 5–12 h for phospholipids and 6–28 h for surfactant proteins (6). Thus, the lung surfactant provides a certain stability to ensure a constant coverage of the alveolar interface and confers it with high flexibility that enables rapid material exchange and adaptation to folding dynamics.

Analysis of lung lavage has revealed that 85–90% of the pulmonary surfactant is composed of lipids, especially dipalmitoylphosphatidylcholine (DPPC), phoshatidylglycerols (PGs), and other mainly unsaturated phospholipids in addition to fatty acids, cholesterol, and proteins (7). The net uncharged and saturated lipid DPPC is primarily responsible for reducing surface tension and withstanding high surface pressures (8). However, it functions poorly in the lung when used alone, apparently because it adsorbs slowly to the air/liquid interface (9). In contrast, negatively charged PGs in the monolayer and in vesicular structures present in the alveolar aqueous hypophase are most relevant for monolayer respreading and enhancement of lipid adsorption from vesicles (10). Also, unsaturated phospholipids have been shown to be good fluidizers and so spread more rapidly to the air/liquid interface due to their low phase transition temperature; their monolayers, however, collapse readily at surface pressures well below those attained under in vivo conditions (11,12). As described by the ''squeeze-out'' theory of lung surfactant function, fluidizing lipids facilitate the adsorption of surfactant molecules to the interface and are selectively removed or squeezed out of the surface layer at higher surface pressure. Thus, the remaining monolayer is probably enriched in lipids that promote low surface tension (13,14).

In addition to the unsaturated phospholipids, the two hydrophobic surfactant-specific proteins SP-B and SP-C are thought to be responsible for rapid protrusion formation and material exchange in the surface layer (13–15). The cysteine-linked homodimer SP-B is composed of 79 amino acids and has a molecular mass of 8.7 kDa. It induces bilayer contact sites and subsequent lipid mixing between bilayers (16,17). SP-B is a protein in pulmonary surfactant that is, in large part, responsible for the prevention of pulmonary alveoli collapse. In addition, its function-determining regions lie in the hydrophilic and hydrophobic domains (18). The 4.2-kDa surfactant protein SP-C consists of 35 amino acids and is one of the most hydrophobic proteins known due to its high content of Val, Ile, and Leu. SP-C stabilizes protrusion formation during exhalation by anchoring the surface monolayer and the underlying multilayers with its palmitoyl residues and α-helix (2,19,20), but it also enhances adsorption of vesicle lipids (10,21,22). It has also been observed that SP-B or SP-C present in DPPC, DPPG, or mixed lipid monolayers alter the thermodynamic properties of the phospholipid membranes (23).

Submitted February 7, 2008, and accepted for publication March 20, 2008.

Address reprint requests to H.-J. Galla, Institute of Biochemistry, Wilhelm-Klemm-Straße 2, 48149 Münster, Germany. Tel.: 0049-251-833200; Fax: 0049-251-8333206; E-mail: gallah@uni-muenster.de.

Editor: Peter Hinterdorfer.

0006-3495/08/07/699/11 $2.00

doi: 10.1529/biophysj.108.131102

Adsorption of vesicle lipids to the interfacial monolayer should occur in distinct steps. Several models have been postulated to describe the mechanism of lipid adsorption (24–26). A two-step model was proposed suggesting transport of vesicles to the surface followed by fusion with the interfacial monolayer (27). However, details of the insertion process still remain uncertain and are a matter of discussion.

In this study, we aimed at further unraveling the mechanistic aspects of lipid adsorption and determining the effect of saturation grade as well as headgroup charge of the phospholipids on the SP-B/SP-C-induced fusion process. Our results are summarized in a detailed model describing distinct steps during the adsorption process.

MATERIAL AND METHODS

Materials

1,2-Dipalmitoyl-*sn*-glycero-3-phosphocholine (DPPC), 1-palmitoyl-2-oleoyl-*sn*-glycero-3-phosphocholine (POPC), 1,2-dipalmitoyl-*sn*-glycero-3-phosphoglycerol (DPPG), and 1-palmitoyl-2-oleoyl-*sn*-glycero-3-phosphoglycerol (POPG) were purchased from Avanti Polar Lipids (Alabaster, AL) and used without further purification. Chloroform and methanol were high-performance liquid chromatography grade and purchased from Sigma-Aldrich (Steinheim, Germany) and Merck (Darmstadt, Germany), respectively. The buffer solution used to hydrate lipid films consisted of *N*-2-(hydroxyethyl)piperazine-*N*′-2-ethansulfonic acid (HEPES) from Merck supplemented with sodium salt of ethylenediaminetetraacetic acid (Na-EDTA) from Sigma-Aldrich. The subphase buffer contained HEPES as well as calcium chloride dihydrate from Fluka (Neu-Ulm, Germany). 2-(4,4-Difluoro-5-methyl-4-bora-3a,4a-diaza-s-indacene-3-dodecanoyl)-1-hexadecanoyl-*sn*-glycero-3-phosphocholine (BODIPY-PC) was obtained from Molecular Probes (Eugene, OR). The preparation of vesicles was carried out with a mini-extruder from Avestin (Liposofast; Ottawa, Canada). The porcine surfactant proteins SP-B and SP-C were purified from bronchoalveolar lavage fluid by butanol extraction (28). The proteins were free of contaminants as was evidenced by electrospray ionization mass spectrometry. The amino acid sequences corresponded to the expected sequences according to the Swiss-Prot database.

Vesicle preparation

A DPPC/DPPG mixture with a molar ratio of 4:1 was dissolved in chloroform/methanol (1:1, v/v) and dried under a stream of nitrogen at 50°C. The remaining solvent was removed for at least 3 h at 50°C in a vacuum oven. The lipid films were hydrated by adding a buffer containing 25 mM HEPES and 0.1 mM Na-EDTA. The vesicle suspension (5 mM) was maintained at 50°C in a water bath for 10 min and was vortexed for 30 s. The procedure of heating and vortexing was repeated twice. The resulting multilamellar vesicles were converted into small unilamellar vesicles at 50°C by membrane extrusion using a polycarbonate membrane with a pore diameter of 50 nm.

Kinetic studies

The kinetic experiments were performed using a preformed monolayer composed of DPPC, DPPG, POPC, or POPG. For lipid/protein films, a protein content of 0.2 mol % for SP-B and 0.4 mol % for SP-C was chosen in accordance with previous investigations (2,20,29–31) and because the content of hydrophobic proteins has been found to be $<1\%$ in lung lavages (9,22). The monolayer was spread at the air/water interface of a Wilhelmy film balance with a 25 ml Teflon trough (15.4 cm $\times$ 2.5 cm) by depositing a few droplets of chloroform/methanol containing the dissolved lipids onto the aqueous surface. The subphase consisted of 25 mM HEPES (pH 7.0) and 3 mM $CaCl_2$ and was stirred continuously by a magnetic bar. The monolayer was compressed with a computer-controlled barrier to a defined surface pressure between 5 mN/m and 45 mN/m. After a constant pressure had been maintained for 10 min, vesicle suspensions were injected through an injection port into the subphase with a Hamilton syringe. The final lipid concentration in the subphase was 20 μmol/L. Insertion of lipids was studied at 20°C by following the surface pressure change with time at constant total area over a time period of at least 7000 s (2 h). The insertion velocity was quantified by determining the initial slope of the pressure-area isotherm.

Kinetic fluorescence microscopy measurements

Fluorescence microscopy images were obtained before and during DPPC/DPPG 4:1 vesicle insertion into a DPPC/SP-C (0.4 mol % of protein) and DPPC/SP-B (0.2 mol % of protein) monolayer on a subphase containing 25 mM HEPES and 3 mM $CaCl_2$. The experimental setup consisted of a light microscope equipped with an XY stage (Olympus BX-FLA; Olympus, Hamburg, Germany) that was connected to a charge-coupled device camera (Hamamatsu, Herrsching, Germany). Phospholipid samples used to form the monolayer were dissolved in chloroform/methanol solvent and doped with 0.1 mol % BODIPY-PC.

RESULTS

The aim of this study was to systematically work out the influence of saturation grade and headgroup charge of phospholipids on the insertion of vesicular material into surfactant model systems spread at the air/water interface of a film balance. We used pure lipid vesicles to mimic the insertion of new surfactant material into the alveolar surface monolayer during inhalation. The presence of negatively charged lipid in the vesicular material and buffered systems containing Ca^{2+} ions in the subphase have previously been reported to be crucial for successful material insertion (10). Moreover, the presence of calcium is essential to mimic the physiological conditions. Unilamellar vesicles were shown to be excellent membrane models to study transport and insertion processes in biomembranes (32). Vesicle insertion dynamics was therefore determined in this study by using unilamellar vesicles with a diameter of 50 nm consisting of DPPC/DPPG (4:1, mol ratio) and surfactant monolayers differing in their lipid and protein composition.

Protein-free monolayers

First, the insertion kinetics of pure lipid systems varying in their saturation grade and headgroup charge was studied. Pressure-time isotherms obtained for DPPC, POPC, DPPG, and POPG monolayers on a buffered subphase (25 mM HEPES, 3 mM $CaCl_2$, pH 7) after addition of DPPC/DPPG 4:1 vesicle at 20°C are presented in Fig. 1. All monolayers were compressed to a defined initial surface pressure before addition of vesicular material into the subphase. The time of vesicle injection is marked with an arrow in the figure.

DPPC monolayers were compressed to different initial surface pressures to study the influence of lipid packing on the insertion process. No sign of pressure increase after vesicle addition was detectable over the entire time range of the

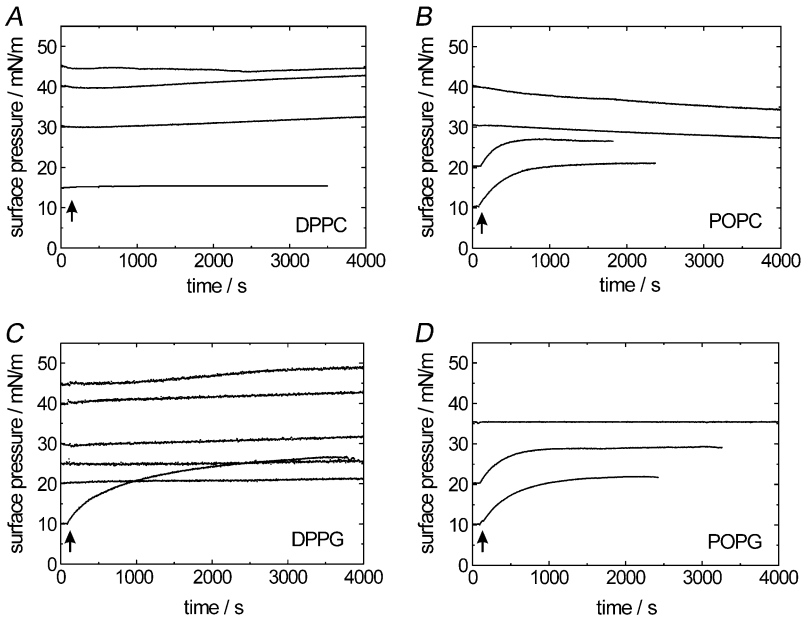

FIGURE 1 Pressure-time isotherms of (*A*) DPPC, (*B*) POPC, (*C*) DPPG, and (*D*) POPG monolayers compressed to different initial surface pressures after injection of DPPC/DPPG 4:1 vesicles into the subphase containing 25 mM HEPES, 3 mM $CaCl_2$ (pH 7) at 20°C. The arrows indicate the time of vesicle injection.

experiment (Fig. 1 *A*). However, when unsaturated and uncharged POPC monolayers were used, a pressure increase of 7–10 mN/m was observable at initial pressures of 10 and 20 mN/m (Fig. 1 *B*). The velocity of vesicle insertion was calculated to be 0.027 ± 0.002 mN/m·s at 10 mN/m and 0.025 ± 0.002 mN/m·s at 20 mN/m, respectively. When the POPC film was compressed to higher start pressures, no pressure increase was discernible. Instead, surface pressure continuously decreased over time, which is indicative of a certain instability of the POPC system.

Monolayers of DPPG that were compressed to initial surface pressures between 20 and 45 mN/m did not exhibit a significant pressure increase after vesicle injection. They remained stable over the entire timescale of the experiment. Unlike DPPC, a pressure increase of ~15 mN/m was observed at an initial pressure of 10 mN/m with an insertion rate of 0.023 ± 0.001 mN/m·s. In the case of POPG, a pressure increase at initial surface pressures of 10 mN/m and 20 mN/m, comparable to those of the POPC system, were visible. The pressure increase was in the range of 8–12 mN/m, and the insertion velocity was 0.024 ± 0.001 mN/m·s at 10 mN/m and 0.027 ± 0.001 mN/m·s at 20 mN/m. Interestingly, POPG monolayers were more stable than those of fluid POPC at an initial pressure of 35 mN/m and did not show any sign of pressure decrease over time.

In summary, saturated lipid monolayers did not display any pressure increase after addition of vesicles to the subphase in the absence of surfactant proteins. One exception was DPPG compressed to an initial pressure of 10 mN/m. Unsaturated monolayers, however, were characterized by a significant pressure increase at low initial pressures (<30 mN/m) after vesicle injection. There was no observable pressure increase only when POPC and POPG monolayers were compressed to initial surface pressures of 30 mN/m and above. In fluid systems, negatively charged monolayers seemed to convey enhanced monolayer stability.

SP-C-containing monolayers

Surfactant specific proteins SP-B and SP-C play an important role in the dynamics of lung surfactant (33). They promote absorption of lipids from membrane suspensions to pure or monolayer-covered air/water interfaces (10,34,35) and induce controlled squeeze-out of surface material during monolayer compression (2,20). In our experiments, we wanted to determine the influence of lipid saturation grade and headgroup charge on surfactant protein-induced material insertion. First, pressure-time isotherms of DPPC/DPPG 4:1 vesicle insertion into DPPC, POPC, DPPG, and POPG monolayers containing 0.4 mol % SP-C on a buffered subphase at 20°C were monitored (Fig. 2).

In contrast to the pure DPPC system, a pronounced pressure increase was already observed in the presence of SP-C at a start pressure of 10 mN/m (Fig. 2 *A*). Below this pressure, no significant pressure increase was detectable. Pressure-time isotherms of DPPC/SP-C monolayers obtained at initial pressures between 10 mN/m and 20 mN/m first showed a lag phase with a very slow pressure increase after vesicle injection. The initial insertion velocity at start pressures of 10, 15, and 20 mN/m were 0.010 ± 0.001 mN/m·s, 0.026 ± 0.001 mN/m·s, and 0.048 ± 0.001 mN/m·s, respectively. As soon as a critical pressure between 20 mN/m and 25 mN/m was exceeded during the time course of the experiment, insertion velocity increased to ~20–30-fold and led to a sigmoidal curve progression. When monolayers were already compressed to initial pressures of 25 mN/m and above, pressure-time isotherms were characterized by an immediate exponential pressure increase after addition of vesicular material.

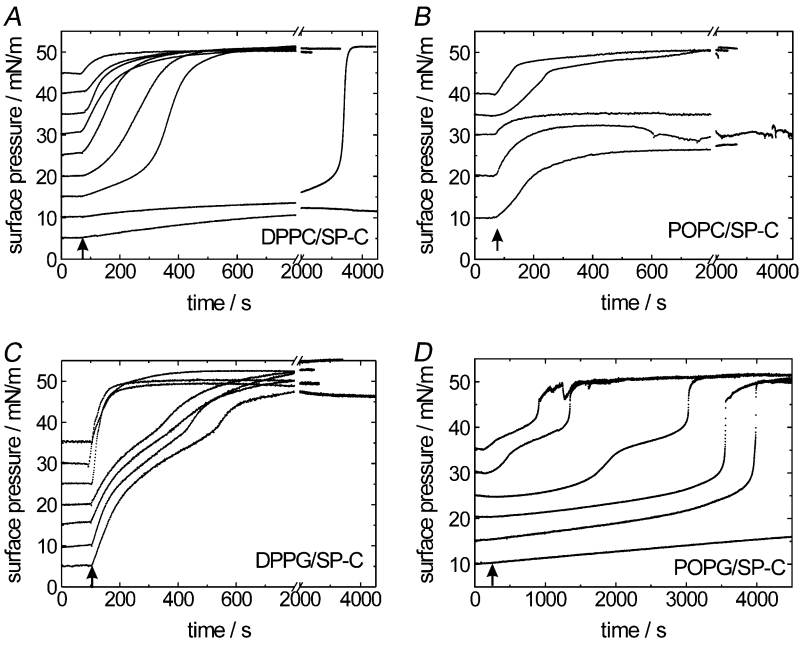

FIGURE 2 Pressure-time isotherms of (*A*) DPPC/SP-C, (*B*) POPC/SP-C, (*C*) DPPG/SP-C, and (*D*) POPG/SP-C monolayers with 0.4 mol % SP-C compressed to different initial surface pressures after injection of DPPC/DPPG 4:1 vesicles into the subphase containing 25 mM HEPES, 3 mM $CaCl_2$ (pH 7) at 20°C. The arrows indicate the time of vesicle injection.

Initial insertion velocities were then at 0.080–0.150 mN/m·s. All pressure-time isotherms of the DPPC/SP-C system (except the one at a start pressure of 5 mN/m) attained a stable equilibrium pressure of 50–52 mN/m.

The insertion process observed for POPC/SP-C systems is characterized by an exponential rather than a sigmoidal pressure increase with pressure changes ranging from 4 mN/m (at an initial pressure of 30 mN/m) to 12 mN/m (at an initial pressure of 10 mN/m). Determination of reproducible initial insertion velocities was hampered due to high monolayer instability. In addition, equilibrium surface pressures reached at the end of the insertion process were different for every initial surface pressure tested. Only the POPC/SP-C isotherms at 35 mN/m and 40 mN/m reached an equilibrium pressure of 50–52 mN/m. As was the case for pure POPC films, reduced monolayer stability led to occasional pressure drops during the measurement.

The isotherms of DPPG/SP-C monolayers most interestingly exhibited a biphasic pressure increase at initial pressures of 5–20 mN/m (Fig. 2 *C*). The first phase was characterized by a pressure increase up to a value of 35 mN/m. The insertion velocities were in the range of 0.194 ± 0.002 mN/m·s (at an initial pressure of 5 mN/m) and 0.130 ± 0.003 mN/m·s (at an initial pressure of 20 mN/m). After a lag phase of 100–150 s, an acceleration of the insertion process was detectable, leading to a second pressure increase up to a final equilibrium surface pressure between 46 mN/m and 53 mN/m. Above an initial pressure of 25 mN/m, only a monophasic behavior was observable. The insertion velocities found for DPPG/SP-C systems at initial pressures above 25 mN/m were ~2.5 times higher than those obtained for lower start pressures and up to 5 times higher compared to the insertion velocities of DPPC/SP-C isotherms at start pressures of 25–45 mN/m.

The pressure-time curves obtained for POPG/SP-C monolayers revealed that pronounced vesicle insertion only occurred at initial surface pressures above 15 mN/m (Fig. 2 *D*). At pressures below 15 mN/m, only a slight increase of 8 mN/m was observed within 7000 s. At initial pressures of 15 and 20 mN/m, a long lag phase followed by a fast pressure increase was observed when a critical pressure of 20–25 mN/m was surpassed in the course of the experiment. Insertion rates were in the range of a biphasic insertion process; however, this was visible only after an initial pressure of 25–35 mN/m. The first pressure increase went up to a value of 35 mN/m, whereas the second one ended at an equilibrium pressure of 48–51 mN/m. Overall, the POPG/SP-C curves reached their end pressure last compared to all other examined systems containing SP-C.

Fluorescence images were taken of a DPPC/SP-C monolayer compressed to an initial pressure of 15 mN/m to obtain information on the processes taking place at the air/water interface during vesicle insertion and the topological characteristics of the monolayer at different points of the pressure-time curve (Fig. 3). The arrows in the figure indicate the pressure regions from which fluorescence images were obtained. Before vesicle injection, only kidney-shaped, regular domains were visible (Fig. 3 *A*). After addition of vesicles to the subphase, already existing domains assumed a rounder shape and new smaller domains appeared in the monolayer during the lag phase (Fig. 3 *B*). When the insertion process suddenly accelerated at 25 mN/m, a significant decrease in domain size was observable, leading to a regular domain pattern at the inflection point of the isotherm (Fig. 3 *C*). When the equilibrium pressure was reached, the monolayer seemed to consist of fused homogenous domain structures (Fig. 3 *D*).

In summary, insertion of DPPC/DPPG vesicles was clearly induced by SP-C. All binary lipid/protein mono-

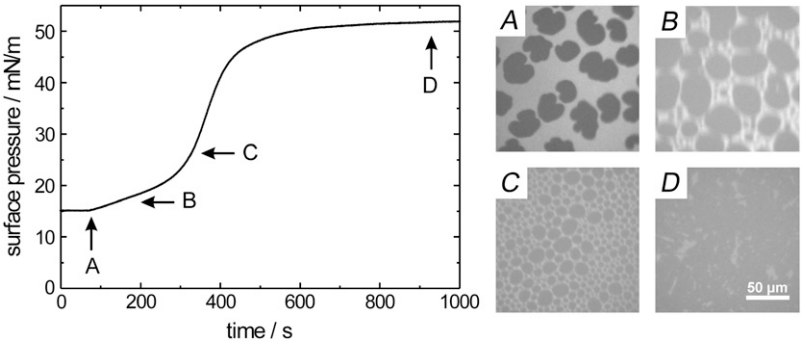

FIGURE 3 Pressure-time isotherm of a DPPC/SP-C monolayer with 0.4 mol % SP-C compressed to 15 mN/m after injection of DPPC/DPPG 4:1 vesicles into the subphase containing 25 mM HEPES, 3 mM $CaCl_2$ (pH 7) at 20°C. Arrows indicate the points on the isotherm at which fluorescence images *A–D* were taken.

layer—except for the POPC/SP-C mixture, which was too unstable—reached an equilibrium surface pressure of 48–51 mN/m. An interesting feature was the appearance of a two-step insertion process only in the presence of PGs and only under conditions with obviously defined molecular packing densities, that is only at <25 mN/m in the presence of saturated DPPG and only at >25 mN/m in fluid POPG layers. Negatively charged lipids again stabilized the monolayer, as was already the case in the protein-free systems.

SP-B-containing monolayers

To determine the influence of SP-B on insertion of DPPC/DPPG 4:1 vesicles into surfactant monolayers containing 0.2 mol % SP-B, lipids differing in headgroup charge and saturation grade pressure-time isotherms were measured (Fig. 4).

Vesicle insertion into DPPC/SP-B monolayers was observable at all investigated initial pressures between 5 and 45 mN/m (Fig. 4 *A*). At start pressures of 5–15 mN/m, curve progression was biphasic. The first phase of vesicle insertion was characterized by an exponential pressure increase of 15–20 mN/m. After a lag time of at least 200 s, the second phase began, leading to another exponential increase up to an equilibrium pressure of 48–52 mN/m. At initial pressures above 25 mN/m, only a monophasic insertion process was identified. All curves reached an end pressure of ~48–52 mN/m. Compared to the SP-C- containing system, 6–28-fold higher insertion velocities at initial pressures of 5–20 mN/m were determined; they ranged from 0.085 mN/m·s to 0.301 mN/m·s at 5 mN/m and 20 mN/m, respectively. At initial pressures above 25 mN/m, however, vesicle insertion into DPPC/SP-B monolayers differed only by a factor of 0.8–2.9 from DPPC/SP-C monolayers and was in the range of 0.104–0.278 mN/m·s.

POPC/SP-B systems proved to by highly unstable, which is the reason that insertion velocities could not be quantified (Fig. 4 *B*). Still, a pronounced SP-B-induced insertion of vesicular material was observable, which ended at different equilibrium pressures. At an initial pressure of 5 mN/m, the POPC/SP-B isotherm rose to an end pressure of 22 mN/m, whereas the curve initially compressed to 10 mN/m showed an end pressure of 40 mN/m.

The insertion of vesicular material into DPPG/SP-B monolayers was characterized by a monophasic insertion process with high insertion velocities that depended on the

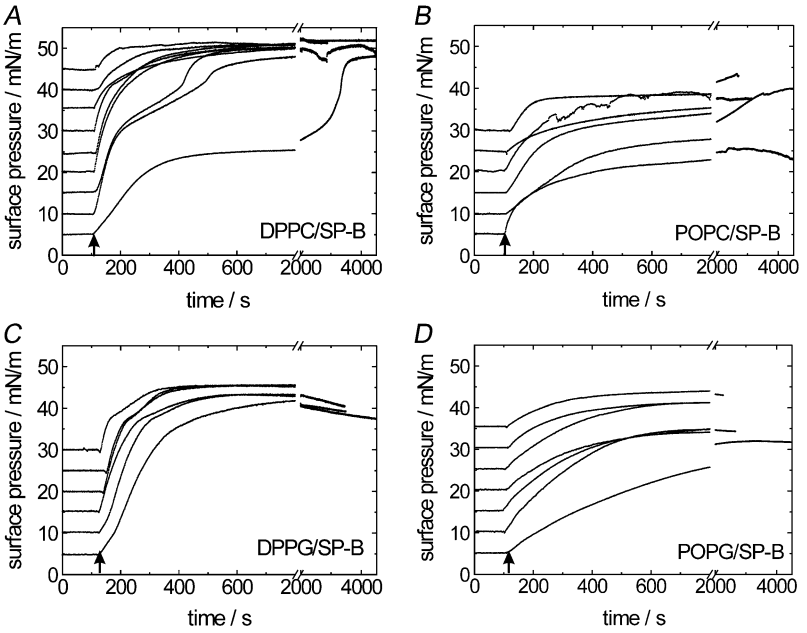

FIGURE 4 Pressure-time isotherms of (*A*) DPPC/SP-B, (*B*) POPC/SP-B, (*C*) DPPG/SP-B, and (*D*) POPG/SP-B monolayers with 0.2 mol % SP-B compressed to different initial surface pressures after injection of DPPC/DPPG 4:1 vesicles into the subphase containing 25 mM HEPES, 3 mM $CaCl_2$ (pH 7) at 20°C. The arrows indicate the time of vesicle injection.

pressure to which the monolayer was first compressed and that were in the same range as in DPPG/SP-C systems. Insertion velocities constantly increased from 0.100 mN/m·s at a start pressure of 5 mN/m to 0.292 mN/m·s at an initial pressure of 30 mN/m (Fig. 4 *C*). All isotherms ended at equilibrium pressures of 40–45 mN/m, which were significantly lower than the ones found for the corresponding SP-C system or the DPPC/SP-B mixture. The presence of negatively charged DPPG, therefore, seems to destabilize the monolayer at higher surface pressures; this can also be seen from the continuous decrease in pressure with time after the equilibrium surface pressure is reached.

Vesicle insertion into POPG/SP-B systems is characterized by an immediate exponential pressure increase at all start pressures tested between 5 mN/m and 35 mN/m (Fig. 4 *D*). Equilibrium pressures, however, demonstrate a high degree of fluctuation and vary from 28 mN/m (at a start pressure of 5 mN/m) to 43 mN/m (at a start pressure of 35 mN/m). Insertion velocities are in the range of 0.046–0.089 mN/m·s.

The fluorescence images taken during material insertion into DPPC/SP-B surface layers reveal a very regular pattern of round domains before vesicle addition to the subphase (Fig. 5 *A*). The first phase of material insertion is characterized by an increase of some of the domains under concomitant change in domain form from round to kidney-shaped (Fig. 5 *B*). During the first lag phase at 40 mN/m, a continuous decrease in domain size is observable (Fig. 5 *C*). At equilibrium pressure, contrast was weak due to self-quenching. Apart from this, the overall appearance of monolayer topology did not change significantly to that observed at 40 mN/m (Fig. 5 *D*).

The kinetic results of SP-B-containing surfactant model systems demonstrate that SP-B also mediates vesicle insertion into preformed monolayers at the air/water interface. Insertion velocities are clearly higher than the ones found for lipid/SP-C mixtures, especially at surface pressures below 25 mN/m. Above this pressure value and in the presence of DPPG insertion, rates were similar to those of SP-C-containing systems. Interestingly, the effect of negatively charged lipids was contrary to the one found for SP-C-containing systems. Biphasic material insertion was only observed for the DPPC/SP-B mixture, whereas two insertion steps were only visible in the presence of PG in SP-C/lipid layers. In addition, PG-containing SP-B monolayers did not withstand or reach high surface pressures of 50 mN/m. Surface layers containing POPC generally proved to be highly unstable in the presence of SP-B and SP-C, which indicates the significance of saturated lipids and negatively charged PGs for surfactant function.

DISCUSSION

Lung surfactant dynamics implies two primary processes: 1), the insertion of new surfactant material from the hypophase into the monolayer lining the alveolar interface and the material squeeze-out for recycling; and 2), the folding and respreading of the meandric surface layers during the breathing cycle. The formation of protrusions from surfactant layers during exhalation was first postulated by von Nahmen et al. (2) upon visualizing three-dimensional structures in Langmuir-Blodgett films of DPPC/DPPG/SP-C monolayers with scanning force microscopy. One year later, Schürch et al. (3) provided proof of multilamellar structures in vivo by transmission electron microscopy of guinea pig lung preparations. The importance of monolayer fluidizing components such as unsaturated POPC and POPG for surfactant dynamics also has been discussed in the context of protrusion formation (4). Unsaturated lipids should enable a fast and especially reversible deconvolution during inhalation because of their nonideal packing and low phase transition temperature (11,12). The squeeze-out theory postulates that fluidizing lipids facilitates the fast adsorption of new material out of the hypophase but that the lipids are easily squeezed out of the surface layer during exhalation. At this stage, only lipids remain in the surfactant layer; these lipids form stable films at high surface pressures and are effective surface tension-reducing agents (13,14,36). In SP-B-containing surfactant model systems, discoidal lipid-protein structures were identified at high surface pressures with scanning force microscopy (20). These SP-B-specific protrusions are considered important for material recycling and surface refinement during the breathing process.

Saturated lipids such as the uncharged DPPC adsorb only very slowly from the hypophase to the monolayer at the air/

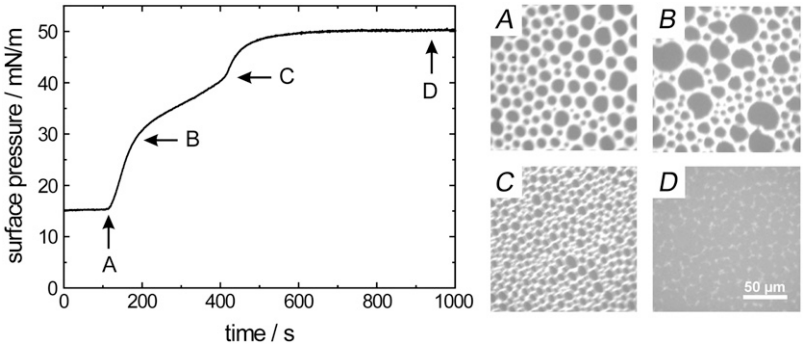

FIGURE 5 Pressure-time isotherm of a DPPC/SP-B monolayer with 0.2 mol % SP-B compressed to 15 mN/m after injection of DPPC/DPPG 4:1 vesicles into the subphase containing 25 mM HEPES, 3 mM $CaCl_2$ (pH 7) at 20°C. Arrows indicate the points on the isotherm at which fluorescence images *A–D* were taken.

water interface (9). It is therefore doubtful that this lipid alone supports the dynamic insertion processes in lung surfactant. Negatively charged lipids, however, evidently accelerate vesicle adsorption (10) and are assumed to play an important role in respreading of surface-confined multilayers (20,37). Yet, the exact role of phospholipid headgroup charge and saturation grade in the material adsorption process has been only insufficiently elucidated thus far.

The two hydrophobic surfactant proteins SP-B and SP-C are known to accelerate dynamic folding and material exchange in the surfactant monolayer (15,34,35,38). SP-B is thought to present the junction between two adjacent lipid layers (16,17), whereas SP-C most probably anchors multilamellar structures to the monolayer and accelerates adsorption of lipid vesicles (2,10,20). Although several protein functions in lung surfactant are already understood, there is no detailed knowledge on specific interactions between these two proteins with individual lipids.

As to the mechanism of the insertion process, the individual steps leading to a controlled refinement of the monolayer are still not understood in detail. Walters et al. (27) proposed a two-step model of adsorption describing the transport of surfactant protein-containing vesicles to the air/water interface as a first step and the subsequent fusion with the monolayer as a second step. Calcium ions are supposed to accelerate the first process by bridging the headgroups of negatively charged lipids present in both the monolayer and the vesicles. The second step is presumably promoted by the presence of fluid lipids because highly curved intermediate structures are assumed to precede membrane fusion, whereas lipid charge is negligible (27). These results were supported by Rodriguez-Capote et al. (39), who also found that a higher lipid fluidity is beneficial for lipid absorption. Although the model of Walters et al. (27) is a good working hypothesis, it still lacks details on structure-function relationships determining individual steps of the insertion kinetics. This article focuses on the insertion of pure lipid vesicles into protein-containing monolayers. Our results demonstrate evidence of clear-cut differences between SP-B and SP-C and provide a refined model that encompasses the molecular and structural characteristics of both hydrophobic surfactant proteins.

Molecular packing and vesicle insertion

When we studied the protein-free lipid systems, we observed a significant pressure increase at low initial pressures ($<$20 mN/m for DPPG and $<$30 mN/m for POPC and POPG). Only DPPC monolayers did not show any sign of vesicle insertion. These results can be explained by the pronounced rigidity of DPPC and its ability to form highly stable monolayers. As was hypothesized previously, DPPC alone seems to be too rigid to enhance a dynamic material exchange (3,40). The pressure increase after vesicle injection in the unsaturated POPC and POPG monolayers at 10 mN/m and 20 mN/m and in the saturated and negatively charged DPPG surface layers at 10 mN/m is indicative of a considerate material insertion. It may be a consequence of the conical shape of DPPG, POPC, and POPG (4,41,42), which could lead to the formation of defects in the monolayer. Fig. 6 shows this hypothesis and provides a convincing model for the observed pressure increase in extremely fluid monolayers. Ca^{2+} ions most likely attach subphase vesicles to the interfacial monolayer via Ca^{2+} bridges. Low lipid packing densities in the monolayer and disordered chain orientation due to the presence of unsaturated acyl chains could then facilitate the insertion of new material from the subphase. Adsorption of vesicle lipids would only occur as long as lipid molecular packing is low and would level off as headgroup spacing decreases. In the case of POPC and POPG, the limiting pressure for defect-induced material insertion would be 30 mN/m. In DPPG monolayers, however, vesicle insertion only occurs at initial pressures below 15 mN/m and leads to a final pressure of 25 mN/m.

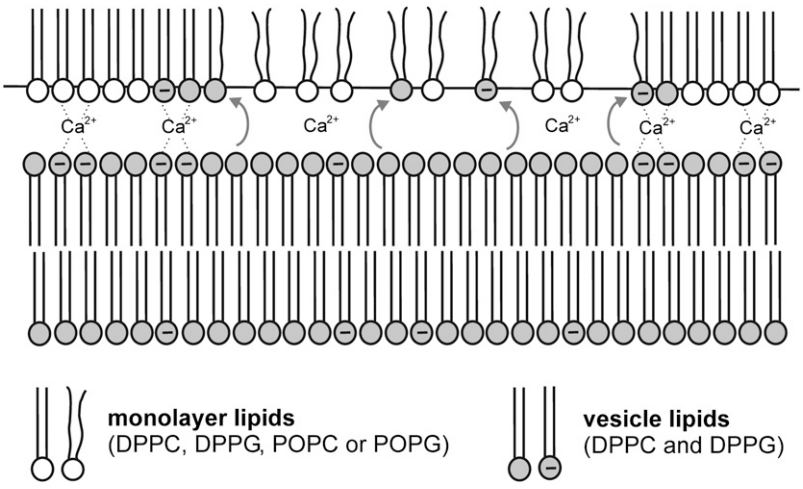

FIGURE 6 Insertion of vesicle lipids into protein-free surface layers. Calcium ions probably induce attachment of vesicles to the surface monolayer by bridging negatively charged lipid phosphate groups. Flip-flop of vesicle lipids could occur in monolayer regions characterized by low lipid packing density and/or disordered chain orientation.

The comparable pressure differences between the start and end pressures obtained for the unsaturated systems suggest that only a certain amount of subphase material enters the surface film. The adsorbed amount of material seems to be higher in the saturated DPPG system than in the two unsaturated ones, which is rather surprising because saturated acyl chains should promote the formation of tightly packed monolayers. Possibly, the presence of calcium ions in the subphase leads to a disturbed packing arrangement where DPPG-Ca^{2+} complexes are most likely to coexist with unbound DPPG molecules. The negative headgroup charges obviously stabilize the monolayers at high surface pressures, as can be seen from the POPG isotherm at 35 mN/m compared to the curve of POPC.

SP-C-induced vesicle insertion

More complex insertion kinetics are observable as soon as the four tested lipid systems are doped with 0.4 mol % SP-C. When only neutral lipids are present in the monolayer, a monophasic insertion process is visible with a sigmoidal or exponential curve progression depending on the initial pressure. It seems that rapid material insertion only occurs when a defined threshold pressure value is exceeded; this is true particularly for lipid/protein mixtures containing saturated lipids or PGs. When negatively charged lipids were mixed with SP-C, insertion velocities increased considerably and, surprisingly, a biphasic insertion mechanism was identified. Insertion velocities depended on the saturation grade and compression state of the monolayer. In the case of DPPG-containing systems, the biphasic process appeared at initial pressures below 25 mN/m; in POPG mixtures, however, an inverse behavior was found, namely the appearance of two insertion steps at initial pressures higher than 25 mN/m. Therefore, it seems that, in the presence of PGs, molecular packing densities have a considerable effect on the insertion mechanism and probably induce a change in protein conformation that significantly enhances material absorption.

We summarized the results obtained from our kinetic measurements in a mechanistic model, which is shown in Fig. 7. From fluorescence measurements performed during the adsorption of vesicle lipids, we concluded that material is first inserted in the fluid regions of the monolayer, because new domains grow in the fluorescent phase representing DPPC in the liquid-expanded state (12). This adsorption step could be similar to the one discussed for the protein-free systems, if we assume that SP-C increases the amount of defects in the monolayer and effectively reduces lipid packing density in the fluid phase (Fig. 7 *A*). As vesicle insertion proceeds and lateral pressure in the monolayer increases, it becomes obvious that SP-C takes a more active role in the adsorption process. SP-C is assumed to be squeezed out of the monolayer upon its compression (30). It is therefore most likely that protrusions formed in this way accelerate material insertion with SP-C connecting neighboring membranes (Fig. 7 *B*). In this manner, the α-helix could penetrate vesicular membranes and disrupt their bilayer structures. Possibly, lipid acyl chains could then change their orientations by hydrophobic interactions with the α-helix and perform an SP-C-mediated flip-flop (Fig. 7 *C*). The presence of negatively charged lipids probably modulates monolayer arrangement and influences the surface pressure at which SP-C is squeezed out of the monolayer. The time constants of the two processes—the molecular packing-induced insertion and the SP-C-triggered adsorption of vesicle lipids—are very likely sensitive to electrostatic interactions and perhaps even specific lipid/protein interactions. Lipid packing density also modulates insertion kinetics. If monolayer stability is too low, as is the case in extremely fluid POPC/SP-C systems, material insertion probably only occurs due to disordered molecular packing and not via the protein-induced adsorption mechanism. Surface films, therefore, must exhibit a minimum stability if SP-C induces rapid material insertion. Further increase in molecular packing by compressing the monolayer above a threshold value of 25 mN/m obviously leads to acceleration of the protein-induced insertion process so that only one insertion step is visible.

SP-B-induced vesicle insertion

Surfactant model systems containing 0.2 mol % SP-B are characterized by insertion rates that are significantly higher than the ones found in the corresponding SP-C mixtures—especially at surface pressures up to 25 mN/m. The only exception was found for DPPG-containing systems. In these systems, insertion velocities were in the pressure range of 5–25 mN/m, which is almost identical to the velocities of DPPG/SP-C monolayers, and only half the value at surface pressures higher than 30 mN/m. POPC-containing monolayers could not be quantified due to high film instability, as was also the case in POPC/SP-C systems.

Even though SP-B effectively induces material insertion at lower surface pressures, a considerable reduction in insertion velocities is observable in the presence of negatively charged lipids as soon as a value of 40 mN/m is exceeded. The slopes of the pressure time curves become less steep above this threshold value, and the final equilibrium pressures reached are well below the value of 50 mN/m that is typical for SP-C-containing monolayers. We could attribute this behavior to SP-B being squeezed out in the presence of PGs at surface pressures of 40 mN/m (20,40) if we assumed that the lipid/protein structures formed in this way were no longer capable of inducing effective material insertion. Differences in protein conformation could also explain these differences in insertion kinetics, especially because the SP-B secondary structure is believed to be very sensitive to electrostatic lipid/protein interactions. For instance, it has been reported that SP-B is less embedded in anionic bilayers than SP-C and probably adopts a more extended conformation, which leads to enhanced recognition by antibodies (43).

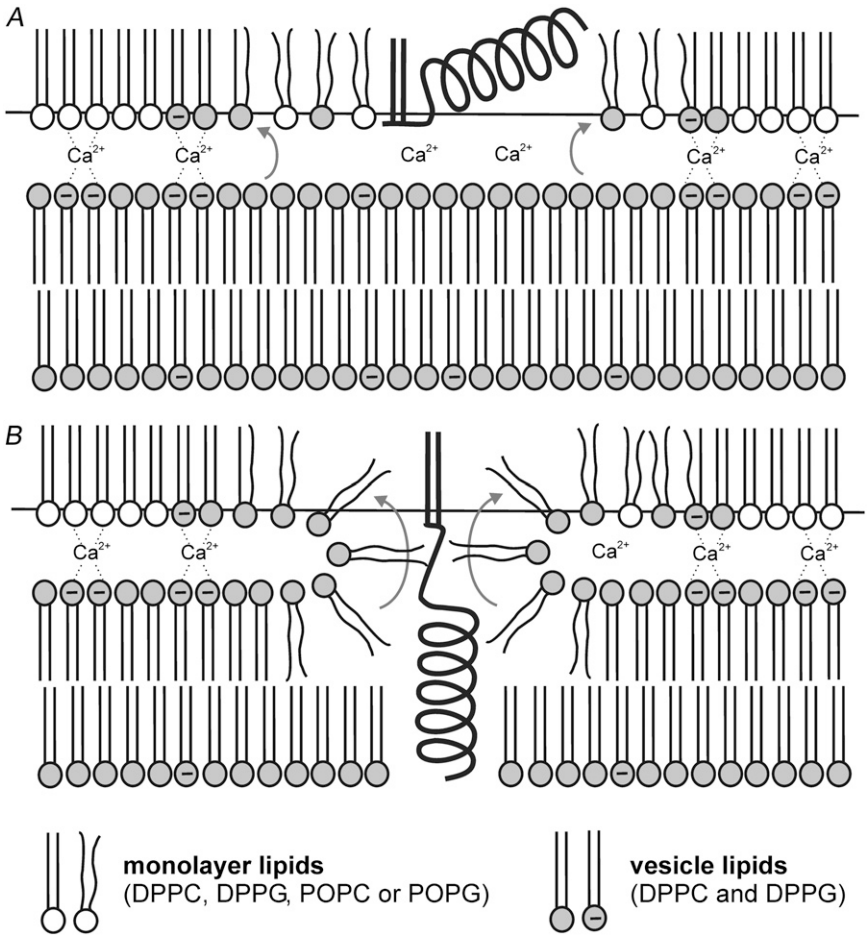

FIGURE 7 Insertion of vesicle lipids into SP-C-containing surface layers. (*A*) Protein-independent lipid insertion into defects created by SP-C. (*B*) SP-C-induced flip-flop of vesicle lipids mediated by hydrophobic interactions. The α-helix of SP-C is inserted into vesicular bilayers, whereas the palmitoyl chains remain in the monolayer.

In contrast to SP-C, biphasic adsorption of vesicle lipids is only monitored in DPPC/SP-B monolayers in the absence of negatively charged lipids and unsaturated acyl chains. This is in clear contrast to SP-C-containing monolayers that displayed a biphasic material insertion exclusively in the presence of negatively charged lipids. If we assume that two insertion steps also occur in SP-B-containing systems—the first one being attributed to a molecular arrangement-induced insertion and the second to an SP-B-promoted mechanism—negatively charged lipids could accelerate the protein-dependent step thus far so that the pressure time courses only appear monophasic. This hypothesis is shown in Fig. 8 in more detail. Due to its larger molecular dimension, SP-B would be more effective in generating defects in the monolayer. This would explain the significantly higher insertion rates observed at lower surface pressures (Fig. 8 *A*). In addition, SP-B is squeezed out at lower surface pressures than SP-C, a process that seems to be enhanced by negatively charged lipids. Therefore, material insertion would also be initiated at lower pressure threshold values and with higher rates. Because SP-B is less hydrophobic than SP-C and possesses seven positive netto charges, we assume that it promotes a flip-flop of the lipids mainly by its hydrophilic core (Fig. 8 *B*). This SP-B-enhanced insertion mechanism, however, only takes place as long the protein is not completely squeezed out of the monolayer. As soon as a threshold value of 40 mN/m is exceeded, PG-induced exclusion of SP-B/lipid aggregates would lead to a significant slowdown and final stop of material insertion (Fig. 8 *C*). At this stage, the possible function of the protein probably extends to stabilize the multilayer structures formed by vesicle adhesion and to generate a surfactant reservoir capable of rapid respreading to the surface upon inhalation.

CONCLUSION

In this study, the influence of lipid saturation grade and headgroup charge on vesicle insertion into surfactant model systems was systematically studied. The insertion process was quantified and led to the development of a refined kinetic model. The results of this study indicate that two steps are involved in the adsorption of vesicle lipids. First, material insertion into disordered monolayers occurs at lower surface pressures. Increased headgroup spacing facilitating material insertion can be achieved either by unsaturated acyl chains or by surfactant proteins SP-B and SP-C disturbing molecular packing in their microenvironment. Because SP-B is larger than SP-C, it apparently creates more defects in the mono-

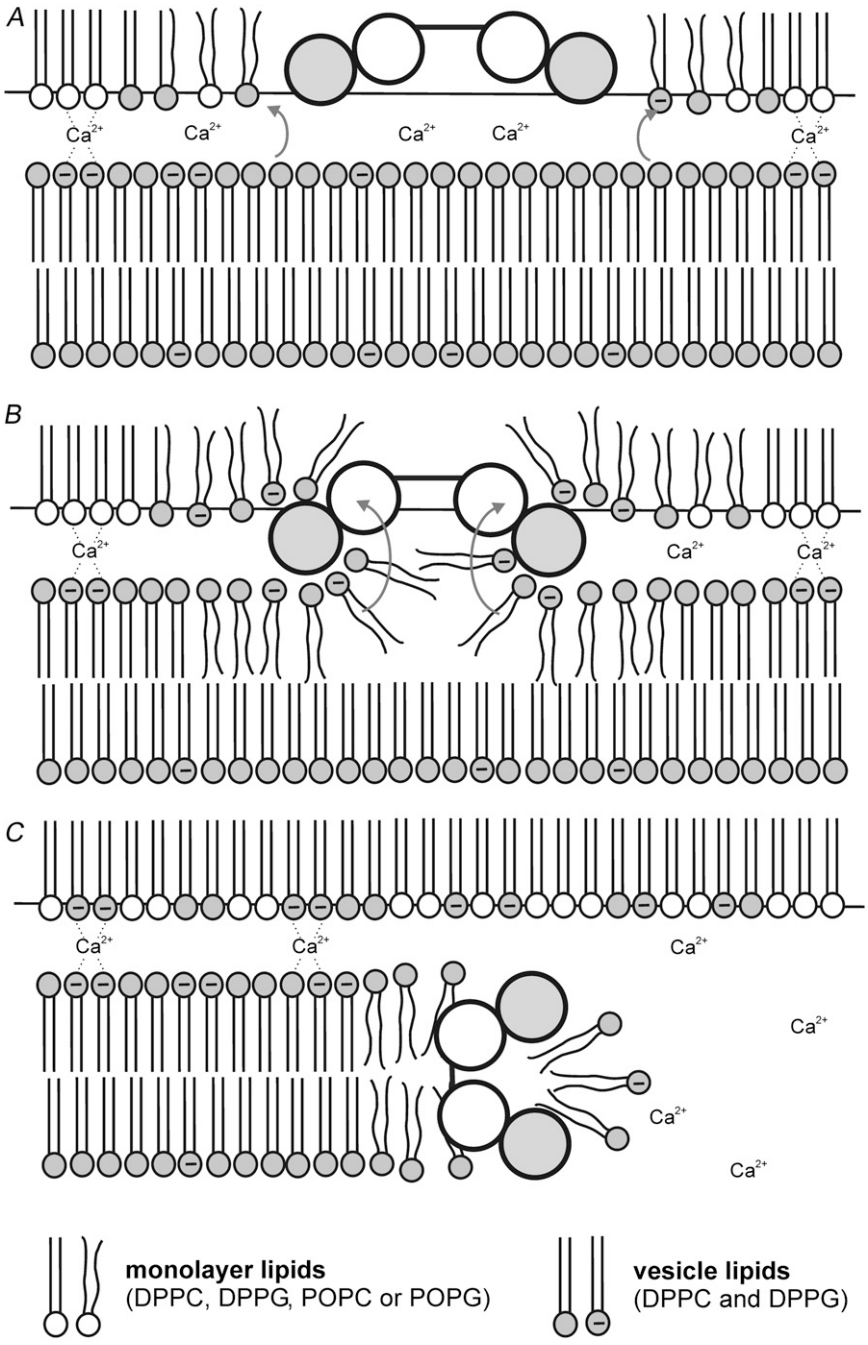

FIGURE 8 Insertion of vesicle lipids into SP-B-containing surface layers. (*A*) Defects caused by the presence of SP-B trigger lipid insertion into the defective monolayer. (*B*) SP-B actively mediates flip-flop of vesicle lipids via hydrophilic interactions. (*C*) Squeeze-out of lipid/SP-B aggregates leads to final stop of lipid insertion at surface pressures exceeding 40 mN/m. Hydrophobic domains of SP-B are colored white, whereas hydrophilic domains are marked in gray.

layer, which leads to higher insertion rates at low initial pressures. The second process is surfactant protein-induced and takes place at higher surface pressures. SP-B and SP-C are successively squeezed out of the monolayer and could act as docking sites for vesicles from the subphase. In addition, they could actively promote vesicle fusion by inducing a flip-flop of lipids to the monolayer. The α-helix of SP-C could enter the vesicle lipid bilayer, which eventually leads to disruption of the bilayer structure and enables the acyl chains to change their orientation by hydrophobic interactions with the α-helix. In the case of SP-B, the outer hydrophilic and positively charged areas of the protein might interact specifically with the negatively charged lipid headgroups. These electrostatic interactions might facilitate the flip-flop of vesicle lipids and thus promote membrane fusion. Specific surfactant protein/PG interactions are also most likely to exist, because negatively charged lipids significantly enhance both SP-C- and SP-B-induced material absorption.

This work was supported by the International North Rhine-Westfalian Graduate School of Chemistry (M.S.) and the Deutsche Forschungsgemeinschaft as a contribution from the Sonderforschungsbereich (424/B9 to H.J.G.).

REFERENCES

1. Schürch, S. 1982. Surface tension at low lung volumes: dependence on time and alveolar size. *Respir. Physiolo. Neurobiol.* 48:339–355.
2. von Nahmen, A., M. Schenk, M. Sieber, and M. Amrein. 1997. The structure of a model pulmonary surfactant as revealed by scanning force microscopy. *Biophys. J.* 72:463–469.
3. Schürch, S., F. H. Y. Green, and H. Bachofen. 1998. Formation and structure of surface films: captive bubble surfactometry. *Biochim. Biophys. Acta.* 1408:180–202.
4. Takamoto, D. Y., M. M. Lipp, A. von Nahmen, K. Y. Lee, A. J. Waring, and J. A. Zasadzinski. 2001. Interaction of lung surfactant proteins with anionic phospholipids. *Biophys. J.* 81:153–169.
5. Piknova, B., V. Schram, and S. B. Hall. 2002. Pulmonary surfactant: phase behavior and function. *Curr. Opin. Struct. Biol.* 12:487–494.
6. Ikegami, M., and A. H. Jobe. 1998. Surfactant protein metabolism in vivo. *Biochim. Biophys. Acta.* 1408:218–225.
7. Possmayer, F., S. H. Yu, J. M. Weber, and P. G. R. Harding. 1984. Pulmonary surfactant. *Can. J. Biochem. Cell Biol.* 62:1121–1133.
8. Schürch, S., J. Goerke, and J. A. Clements. 1976. Direct determination of surface tension in the lung. *Proc. Natl. Acad. Sci. USA.* 73:4698–4702.
9. Hall, S. B., A. R. Venkitaraman, J. A. Whitsett, B. A. Holm, and R. H. Notter. 1992. Importance of hydrophobic apoproteins as constituents of clinical exogenous surfactants. *Am. Rev. Respir. Dis.* 145:24–30.
10. Ross, M., S. Krol, A. Janshoff, and H.-J. Galla. 2002. Kinetics of phospholipid insertion into monolayers containing the lung surfactant proteins SP-B or SP-C. *Eur. Biophys. J.* 31:52–61.
11. McConnell, H. M. 1991. Structures and transitions in lipid monolayers at the air-water interface. *Annu. Rev. Phys. Chem.* 42:171–195.
12. Möhwald, H. 1990. Phospholipid and phospholipid-protein monolayers at the air/water interface. *Annu. Rev. Phys. Chem.* 41:441–476.
13. Pastrana-Rios, B., C. R. Flach, J. W. Brauner, A. J. Mautone, and R. Mendelsohn. 1994. A direct test of the ''squeeze-out'' hypothesis of lung surfactant function. External reflection FT-IR at the air/water interface. *Biochemistry.* 33:5121–5127.
14. Goerke, J. 1998. Pulmonary surfactant: functions and molecular composition. *Biochim. Biophys. Acta.* 1408:79–89.
15. Perez-Gil, J., and K. M. Keough. 1998. Interfacial properties of surfactant proteins. *Biochim. Biophys. Acta.* 1408:203–217.
16. Oosterlaken-Dijksterhuis, M. A., M. van Eijk, L. M. van Golde, and H. P. Haagsman. 1992. Lipid mixing is mediated by the hydrophobic surfactant protein SP-B but not by SP-C. *Biochim. Biophys. Acta.* 1110:45–50.
17. Hawgood, S., M. Derrick, and F. Poulain. 1998. Structure and properties of surfactant protein B. *Biochim. Biophys. Acta.* 1408:150–160.
18. Cochrane, C. G., and S. D. Revak. 1991. Pulmonary surfactant protein B (SP-B): structure-function relationships. *Science.* 254:566–568.
19. Bourdos, N., F. Kollmer, A. Benninghoven, M. Ross, M. Sieber, and H.-J. Galla. 2000. Analysis of lung surfactant model systems with time-of-flight secondary ion mass spectrometry. *Biophys. J.* 79:357–369.
20. Krol, S., A. Janshoff, M. Ross, and H.-J. Galla. 2000. Structure and function of surfactant protein B and C in lipid monolayers: a scanning force microscopy study. *Phys. Chem. Chem. Phys.* 2:4586–4593.
21. Johansson, J. 1998. Structure and properties of surfactant protein C. *Biochim. Biophys. Acta.* 1408:161–172.
22. Curstedt, T., J. Johansson, P. Persson, A. Eklund, B. Robertson, B. Löwenadler, and H. Jörnvall. 1990. Hydrophobic surfactant-associated polypeptides: SP-C is a lipopeptide with two palmitoylated cysteine residues, whereas SP-B lacks covalently linked fatty acyl groups. *Proc. Natl. Acad. Sci. USA.* 87:2984–2989.
23. Shiffer, K., S. Hawgood, H. K. Haagsman, B. Benson, J. A. Clements, and J. Goerke. 1993. Lung surfactant proteins, SP-B and SP-C, alter the thermodynamic properties of phospholipid membranes: a differential calorimetric study. *Biochemistry.* 32:590–597.
24. King, R. J., and J. A. Clements. 1972. Surface active materials from dog lung. III. Thermal analysis. *Am. J. Physiol.* 223:727–733.
25. Davies, R. J., M. Genghini, D. V. Walters, and C. J. Morley. 1986. The behaviour of lung surfactant in electrolyte solutions. *Biochim. Biophys. Acta.* 878:135–145.
26. Ivanova, T., G. Georgiev, I. Panaiotov, M. Ivanova, M. A. Launois-Surpas, J. E. Proust, and F. Puisieux. 1989. Behavior of liposomes prepared from lung surfactant analogues and spread at the air-water interface. *Prog. Colloid Polym. Sci.* 79:24–32.
27. Walters, R. W., R. R. Jenq, and S. B. Hall. 2000. Distinct steps in the adsorption of pulmonary surfactant to an air-liquid interface. *Biophys. J.* 78:257–266.
28. Haagsman, H. P., S. Hawgood, T. Sargeant, D. Buckley, R. T. White, K. Drickamer, and B. J. Benson. 1987. The major lung surfactant protein, SP 28–36, is a calcium-dependent, carbohydrate-binding protein. *J. Biol. Chem.* 262:13877–13880.
29. Amrein, M., A. von Nahmen, and M. Sieber. 1997. A scanning force- and fluorescence light microscopy study of the structure and function of a model pulmonary surfactant. *Eur. Biophys. J.* 26:349–357.
30. Galla, H.-J., N. Bourdos, A. von Nahmen, M. Amrein, and M. Sieber. 1998. The role of pulmonary surfactant protein C during the breathing cycle. *Thin Solid Films.* 327–329:632–635.
31. von Nahmen, A., A. Post, H.-J. Galla, and M. Sieber. 1997. The phase behavior of lipid monolayers containing pulmonary surfactant protein C studied by fluorescence light microscopy. *Eur. Biophys. J.* 26:359–369.
32. Szoka, F. Jr., and D. Papahadjopoulos. 1978. Procedure for preparation of liposomes with large internal aqueous space and high capture by reverse-phase evaporation. *Proc. Natl. Acad. Sci. USA.* 75:4194–4198.
33. Batenburg, J. J., and H. P. Haagsman. 1998. The lipids of pulmonary surfactant: dynamics and interactions with proteins. *Prog. Lipid Res.* 37:235–276.
34. Oosterlaken-Dijksterhuis, M. A., H. P. Haagsman, L. M. van Golde, and R. A. Demel. 1991. Interaction of lipid vesicles with monomolecular layers containing lung surfactant proteins SP-B or SP-C. *Biochemistry.* 30:8276–8281.
35. Oosterlaken-Dijksterhuis, M. A., H. P. Haagsman, L. M. van Golde, and R. A. Demel. 1991. Characterization of lipid insertion into monomolecular layers mediated by lung surfactant proteins SP-B and SP-C. *Biochemistry.* 30:10965–10971.
36. Watkins, J. C. 1968. Surface properties of pure phospholipids in relation to those of lung extracts. *Biochim. Biophys. Acta.* 152:293–306.
37. Pérez-Gil, J. 2001. Lipid-protein interactions of hydrophobic proteins SP-B and SP-C in lung surfactant assembly and dynamics. *Pediatr. Pathol. Mol. Med.* 20:445–469.
38. Schram, V., and S. B. Hall. 2001. Thermodynamic effects of the hydrophobic surfactant proteins on the early adsorption of pulmonary surfactant. *Biophys. J.* 81:1536–1546.
39. Rodriguez-Capote, K., K. Nag, S. Schürch, and F. Possmayer. 2001. Surfactant protein interactions with neutral and acidic phospholipid films. *Am. J. Physiol. Lung Cell. Mol. Physiol.* 281:L231–L242.
40. Serrano, A. G., and J. Pérez-Gil. 2006. Protein-lipid interactions and surface activity in the pulmonary surfactant system. *Chem. Phys. Lipids.* 141:105–118.
41. Saulnier, P., F. Foussard, F. Boury, and J. E. Proust. 1999. Structural properties of asymmetric mixed-chain phosphatidylethanolamine films. *J. Colloid Interface Sci.* 218:40–46.
42. Malcharek, S., A. Hinz, L. Hilterhaus, and H.-J. Galla. 2005. Multilayer structures in lipid monolayer films containing surfactant protein C: effects of cholesterol and POPE. *Biophys. J.* 88:2638–2649.
43. Oviedo, J. M., C. Casals, and J. Pérez-Gil. 2001. Pulmonary surfactant protein SP-B is significantly more immunoreactive in anionic than in zwitterionic bilayers. *FEBS Lett.* 494:236–240.